IEEE Photonics Journal
An IEEE Photonics Society Publication

Open Access

Temperature Sensor Based on Photonic Crystal Fiber Filled With Liquid and Silver Nanowires

Volume 8, Number 3, June 2016

X. C. Yang
Y. Lu
B. L. Liu
J. Q. Yao

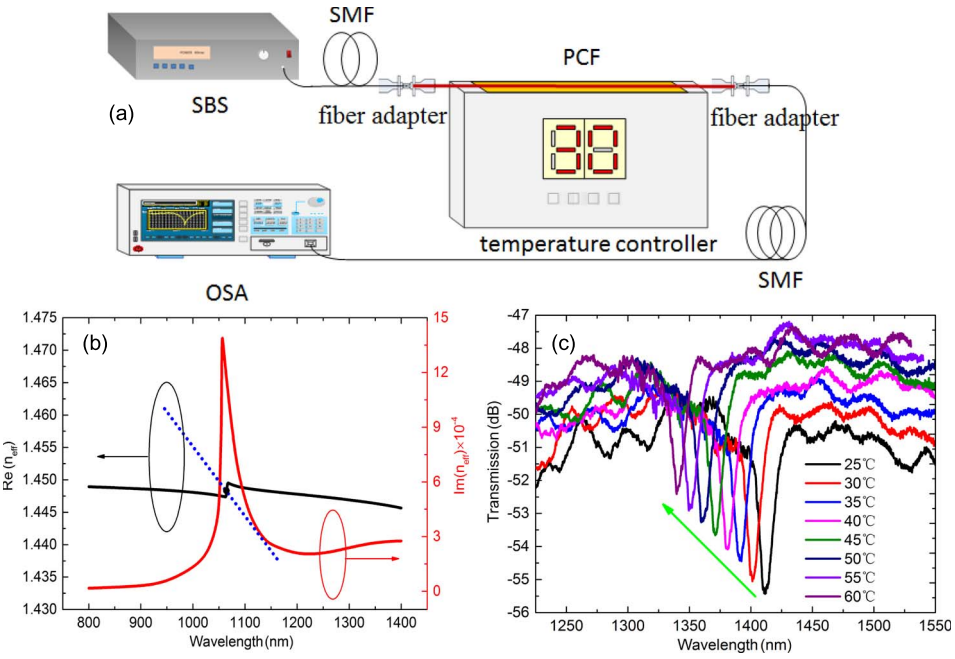

DOI: 10.1109/JPHOT.2016.2568101
1943-0655 © 2016 IEEE

IEEE photonics SOCIETY

IEEE

Temperature Sensor Based on Photonic Crystal Fiber Filled With Liquid and Silver Nanowires

X. C. Yang, Y. Lu, B. L. Liu, and J. Q. Yao

Institute of Laser and Opto-Electronics, College of Precision Instrument and Opto-electronics Engineering, Key Laboratory of Opto-Electronics Information Technology (Ministry of Education), Tianjin University, Tianjin 300072, China

DOI: 10.1109/JPHOT.2016.2568101

Manuscript received April 21, 2016; revised May 6, 2016; accepted May 9, 2016. Date of publication May 12, 2016; date of current version May 31, 2016. This work was supported by the National Basic Research Program of China (973 Program) under Grant 2010CB327801. Corresponding author: Y. Lu (e-mail: luying@tju.edu.cn).

Abstract: A temperature sensor based on photonic crystal fiber filled with liquid and silver nanowires using surface plasmon resonance is demonstrated both theoretically and experimentally in this paper. Numerical simulation shows that a blue shift is obtained when temperature increases, and the resonance wavelength and resonance intensity can be tuned effectively by adjusting the volume ratios of the liquid constituents. A large temperature range from 25 °C to 60 °C at different ratios is detected to investigate the sensor's performance, and the sensitivity –2.08 nm/°C with the figure of merit of 0.1572 is obtained by experiment. Moreover, with the all-fiber device with strong mechanical stability, it is easy to realize remote sensing by changing the downlead fiber length, which is promising for developing a high-sensitive, real-time, and distributed temperature sensor.

Index Terms: Temperature sensor, photonic crystal fiber, surface plasmon resonance, silver nanowires.

1. Introduction

The photonic crystal fiber (PCF) is a particular kind of fiber based on the method of 2-D photonic crystals and consists of a periodical array of air holes extending along the whole fiber length [1]. The flexible design of PCF provides many advantages compared with conventional optical fiber, such as single mode propagation, high confinement, controllable birefringence, low non-linearity, etc. [2]. Additionally, the existence of air holes provides the possibility to insert functional materials [3], which can realize the interaction of transmission light and materials effectively. Recently, a large variety of PCF based sensors are reported to measure temperature [4]–[8], strain [9], vibration [10], twist [11], refractive index (RI) [12], [13], gas absorption [14], magnetic field [15], and so on, which have been widely used in physical, chemical, and biochemical sensing applications.

Surface plasmon resonance (SPR) is the excitation of a charge density oscillation (surface plasmons, SPs) caused by a p-polarized light along the metal-dielectric interface by satisfying phase matching condition between p-polarized light and SPs. SPR technique owns extraordinary properties like label free, real-time and high resolutions down to 10^{-7} RI units (RIUs) [16],

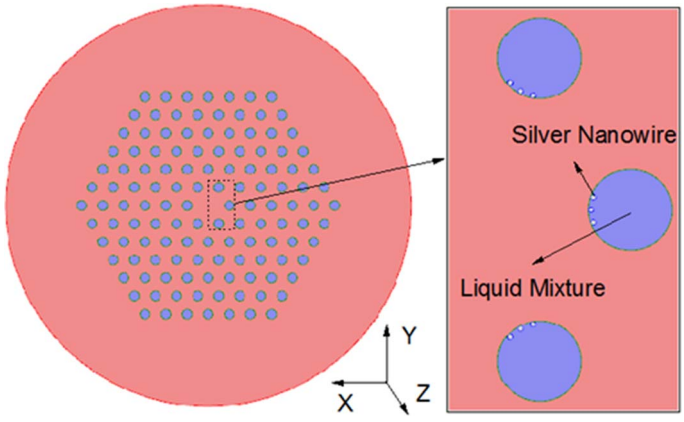

Fig. 1. Schematic of the designed sensor filled with liquid and silver nanowires.

which is not accessible to other sensing methods. Combining the advantages of PCF and SPR, many sensing devices have been very recently reported [12], [13], [17]–[19]. Hassani *et al.* first designed a RI sensor and realize the detectable RI change of 10^{-4} [17]. Peng *et al.* proposed a temperature sensor based on SPR within selectively coated PCF, and the sensitivity 720 pm/°C is obtained [18]. Liu *et al.* presented a same type sensor based on PCF coated with nanoscale gold film. By removing air holes in the second layer, the coupling between core mode and SP polariton (SPP) mode occurs easily, and the average sensitivity obtained is –2.15 nm/°C [19], but they are all based on the numerical simulations, and the coating operation is quite difficult to realize experimentally.

To solve the metal film coating problem, some researchers proposed metal nanoparticles filled sensors. In [20], Csaki *et al.* demonstrated a nanoparticle layer deposition method using self-assembled monolayer technique and the RI sensitivity 78 nm/RIU is measured experimentally. By filling gold nanoparticles and dimethyl sulfoxide into the holes selectively, Peng *et al.* presented a temperature sensor using bandgap-like effect and the sensitivity is up to –5.5 nm/°C by experiment [21]. Lu *et al.* also reported a silver nanowires filled temperature sensor and realize the sensitivity of 2.7 nm/°C [22]. However, the selectively filling is not easy to operate in [21] and the incident light coupled by lens in [22] reduces the mechanical stability, which will restrict its wide application.

In this paper, an all-fiber temperature sensor based on LMA-10 PCF filled with silver nanowire colloids and chloroform is both analyzed theoretically and demonstrated experimentally. Finite element method (FEM) is utilized though COMSOL Multiphysics software and simulated results show that a blue shift is obtained when temperature increase, the volume fractions of silver nanowire colloids and chloroform have a great influence on the sensor's resonance wavelength and resonance intensity. A large temperature range from 25 °C to 60 °C at the ratios of 1:1 and 1:2 are detected to investigate the sensor's performance and an average sensitivity –2.08 nm/°C with a figure of merit (FOM) of 0.1572 is obtained by experiment. A significant advancement is made compare with the previous work in [22] as the all-fiber structure can strengthen the sensor's mechanical stability and realize the remote sensing. Moreover, we enlarge the range of temperature measurement with narrower measurement interval, the FOM is also increased from less than 0.135 to 0.1572 with little sacrifice in wavelength sensitivity (2.7 nm/°C in [22]), which can improve the detection accuracy significantly.

2. Theoretical Modeling

Fig. 1 shows the schematic of the designed temperature sensor. The fiber cladding consists of six layers air holes of hexagonal lattices. The diameters of the fiber, the core, and the cladding air hole are $D = 125$ *u*m, $d_c = 10$ um, and $d = 3$ um, respectively. The pitch is $\Lambda = 6.5$ um. The

liquid mixture of aqueous silver nanowire colloids and chloroform at the ratio of 1:2 is full-filled into the air holes as the sensing medium by capillary force and air pressure [5]. The silver nanowire colloid we used is a stable translucent colloidal suspension of silver nanowires in ethanol carrier. Then the mixed liquid can be regarded as the mixture of ethanol and chloroform. The diameter of the nanowires is about 90 nm, and the average length is about 30 um. As shown in Fig. 1, some silver nanowires are embedded in the air holes of the first layer in numerical simulation and the distribution of silver nanowires refers to [23], [24]. Lu *et al.* have demonstrated that when the number of silver nanowires embedded in each air hole of the first layer exceeds three, the sensor will get saturated wavelength and amplitude sensitivities. The sensitivities will remain relatively stable with the continuous increasing of the silver nanowires numbers. Luan *et al.* presented that the silver nanowires are unlikely to suspended in the liquid for a long time because of the gravity effect, and the resonance wavelength will not change as long as the nanowires are still on the surfaces of the holes and that sensitivity of the sensor is relatively stable with the randomly filled nanowires.

Finite element method (FEM) is used to calculate the results using COMSOL Multiphysics software. We use perfectly matched layers (PML) as the boundary condition and the whole section of the sensor is divided into many triangular subdomains. The total number of mesh elements is 74262. The simulation for modal analysis is done in XY plane while light propagation is along Z direction.

The RI of mixed liquid made up of silver nanowire colloids and chloroform can be evaluated by [23]

$$\frac{n^2-1}{n^2+2}=\phi_1\frac{n_1^2-1}{n_1^2+2}+\phi_2\frac{n_2^2-1}{n_2^2+2} \tag{1}$$

where n, n_1, and n_2 denote the RI of the liquid mixture and the constituents, respectively. ϕ_1 and ϕ_2 are the volume fractions of the constituents, and ϕ_2 can be replaced by $(1-\phi_1)$. The RI of liquid constituent can be evaluated by [23]

$$n=n_0+\frac{dn}{dT}(T-T_0) \tag{2}$$

where n_0 is the RI of the liquid constituent at temperature T_0 and dn/dT is the thermo-optic coefficient. The thermo-optic coefficients of ethanol and chloroform are $-4\times10^{-4}/^{\circ}\mathrm{C}$ and $-6.328\times10^{-4}/^{\circ}\mathrm{C}$, respectively. The fiber material $(\sim10^{-6}/^{\circ}\mathrm{C})$ and the silver are much lower than the liquid; therefore, we do not take them into consideration. The RIs of ethanol and chloroform $(T=20^{\circ}\mathrm{C})$ are defined as

$$n_{\text{ethanol}}=1.35265+0.00306\lambda^{-2}+0.00002\lambda^{-4} \tag{3}$$

$$n_{\text{chloroform}}=1.431364+0.00563241\lambda^{-2}-2.0805\times10^{-4}\lambda^{-4}. \tag{4}$$

The RI of fiber material is assumed to be 1.45 (fused silica) and the RI of silver refers to the *Handbook of Optics* [25]. The RI relationship between mixed liquid and the background material of PCF with the increase of temperature are shown in Fig. 2, which exhibits a declining trend of mixed liquid and a lower state comparing with fused silica due to the negative thermo-optical coefficients of ethanol and chloroform. Then, the effective RI (n_{eff}) of the cladding is always lower than the n_{eff} of the core, making the total internal reflection sensing mechanism guaranteed.

Fig. 3 shows the dispersion relations of the core guided mode and the plasmon mode at the resonance wavelength. We use the Gaussian-like modes as the core guided modes as it is best suited for the excitation by standard Gaussian laser sources [26]. Theoretically, phase matching requires equating the propagation constants of the core guided mode and the plasmon mode, implying that the n_{eff} of the two modes have to be close. The n_{eff} of core guided mode (black solid line) is close to that of the core material. The n_{eff} of plasmon mode (blue dotted line) is determined by the background silica, the adjacent analyte, and the metallic coating, usually at a

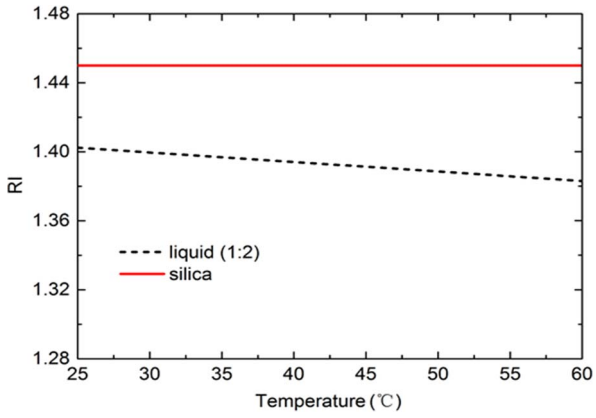

Fig. 2. RI relationship between the mixed liquid and the background material of the PCF with the increase of temperature.

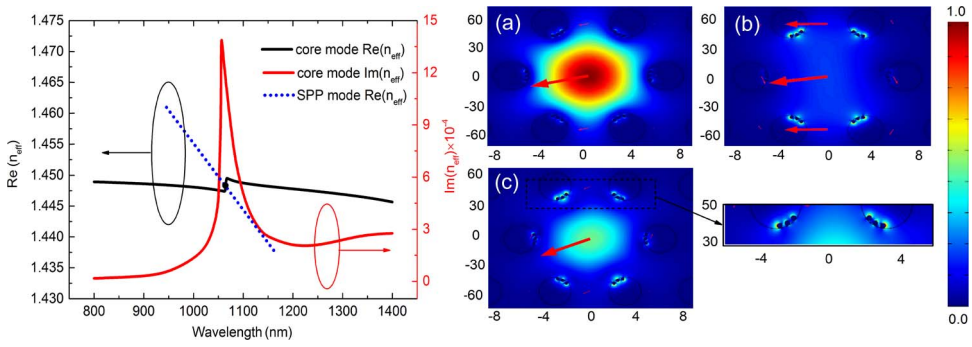

Fig. 3. (Left) Dispersion relations of the core-guided mode and the plasmon mode at the resonance wavelength. (Right) Electric field distributions of the (a) core-guided mode at $\lambda = 800$ nm, (b) plasmon mode at $\lambda = 1075$ nm, and (c) core-guided mode at $\lambda = 1080$ nm (phase-matching point).

value not significantly larger than the filling analyte [27]. Obviously, we can see that when phase matching condition is satisfied at a certain wavelength (intersection point of black and blue line), the energy of the core guided mode is transferred to the plasmon and a resonant loss peak (red solid curve) is observed at this wavelength. As the filling liquid mixture has a large thermo-optic coefficient, temperature variations will change the RI of the filled mixture and influence the coupling efficiency between the core guided mode and the plasmon mode, thus leading to a peak shift. By measuring the peak shift, temperature changes can be detected effectively.

When temperature increases from 30 °C to 60 °C, as shown in Fig. 4(a), the resonance peak shifts to the shorter wavelength and the peak loss decreases gradually. This is because a reduced n_{eff} of the plasmon mode changes the phase matching point and a larger difference between core guided mode and plasmon mode making the coupling efficiency weaker. Contrary to the temperature increasing, varying the volume ratios of ethanol and chloroform from 1:1 to 1:3, as we see from Fig. 4(b), the peak wavelength shifts to the longer wavelength and the peak loss increasing as a larger volume ratio of chloroform leads to an increased n_{eff} of the plasmon mode. However, we should note that a larger volume ratio of chloroform will dilute the silver nanowires. As described in [24], the peak wavelength changes little but the peak loss decreases evidently when the number of silver nanowires in each air hole decreased. In other words, increase the volume ratio of chloroform will also decrease the peak loss. Therefore, by adjusting the volume fractions of the constituents, we can tune the peak wavelength and peak loss intensity to a desired value in the experiment.

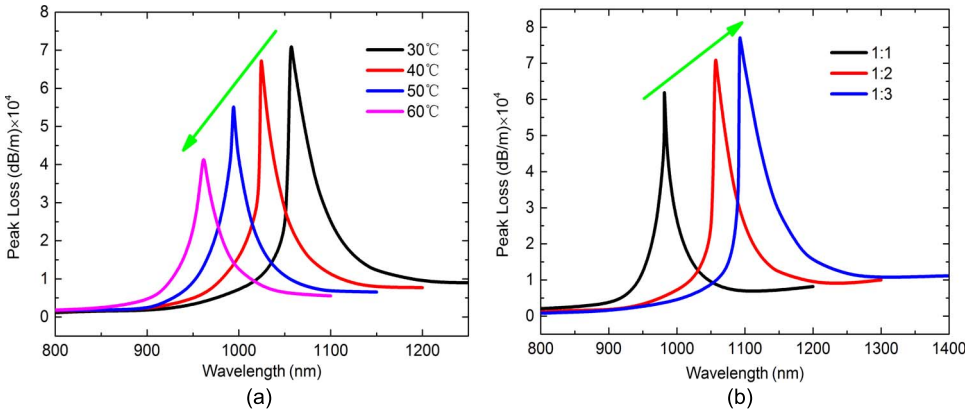

Fig. 4. (a) Loss spectra of the designed sensor when temperatures are 30 °C, 40 °C, and 50 °C. (b) Loss spectra of the designed sensor when volume ratios of ethanol and chloroform are 1:1, 1:2, and 1:3.

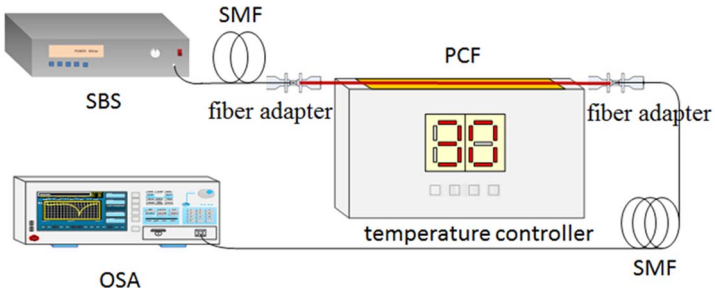

Fig. 5. Scheme of the experimental setup for the designed sensor.

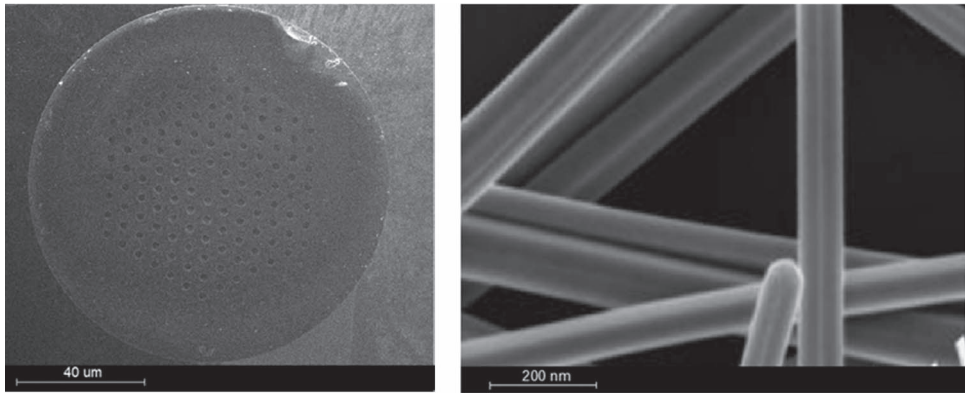

Fig. 6. (a) SEM image of the LMA-10 PCF. (b) SEM image of the silver nanowire.

3. Experimental Setup and Analysis

We design a setup to certify the temperature sensor's feasibility, which is shown in Fig. 5. A supercontinuum broadband source (SBS) (NKT SuperK Compact) is used as the light source and an optical spectrum analyzer (OSA) (YOKOGAWA AQ6370C) is used to monitor the transmission spectrum passing though the single mode fibers (SMFs) and the PCF. The scanning electron microscope (SEM) image of LMA-10 PCF is shown in Fig. 6(a). Two ends of the PCF are connected with the SMFs via bare fiber adapters and then fixed onto a temperature

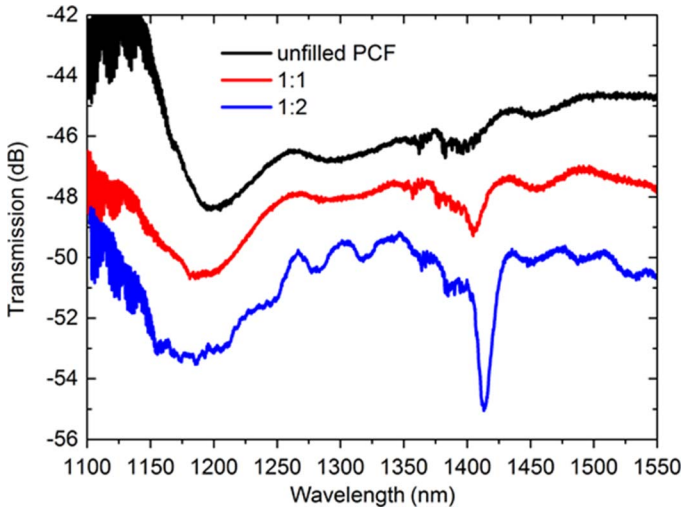

Fig. 7. Transmission spectra of the designed sensor for the unfilled PCF and the liquid-filled PCF with volume ratios 1:1 and 1:2.

controller. The all-fiber sensor is easy to achieve remote sensing by extending the length of the downlead SMF and have a strong mechanical stability compare with the incident light coupled by lens in [22], also the whole structure is more compact. The liquid mixture of aqueous silver nanowire colloids and chloroform at the ratio of 1:2 is full-filled into the air holes of an 8 cm PCF with the well-known capillary action. One end of the PCF is immersed into the liquid while the other end is exposed to the air, then the liquid are full-filled into the air holes by capillary force and air pressure. To save the filling time, we exert pressure on the liquid using a similar setup, as described in [21]. The PCF is fully infiltrated by adding nitrogen gas pressures of ~3 bars for one hour. The silver nanowire colloids we used is a stable translucent colloidal suspension of silver nanowires in ethanol carrier and the concentration is 1000 ppm. The SEM image of silver nanowire is shown in Fig. 6(b).

First, we detect the transmission loss of the sensor for unfilled PCF, liquid filled PCF with volume ratio 1:1 and 1:2 at 30 °C, respectively, which is shown in Fig. 7. Two loss curves are observed when the PCF are filled with the liquid mixture of ethanol and chloroform. Compared with the unfilled PCF, we can know that the curve on the left is caused by the light source and the fiber, which has a larger spectral width and a shallower curve depth than the SPR curve on the right. Moreover, the sensor filled with a larger volume ratio of chloroform exhibits a narrower and deeper loss curve, leading to a higher resolution make the detection much easier and more accurate.

Next, a large temperature range from 25 °C to 60 °C with the steps of 5 °C at the ratio of 1:1 and 1:2 are detected to investigate the sensor's performance. As shown in Fig. 8, with temperature increasing, the resonance wavelengths all blue-shift significantly and the resonance losses damp gradually. In addition, the sensor filled with liquid at the ratio 1:2 exhibits a narrower and deeper loss curve compared with 1:1, which all agree well with the simulated results. The detailed parameters are summarized in Table 1. We should also note that the decreasing resonance dip will widen the spectral width and thus reducing the resolution of the sensor. This phenomenon is attributed to the negative thermo-optic coefficients of ethanol and chloroform. As we see from Fig. 2, the RI of liquid mixture will decrease as temperature increasing. The liquid mixture is filled into the air holes in the fiber cladding, and therefore the n_{eff} of the plasmon mode is close to the RI of the mixture. Hence, the increasing temperature will decrease the n_{eff} of the plasmon mode, leading to the phase matching point shifts to the shorter wavelength. Moreover, the RI of liquid being far from the RI of fiber material (fused silica about 1.45) will enlarge the n_{eff} difference between the core mode and the plasmon mode, thus reducing the coupling efficiency and resulting in lower resonance loss.

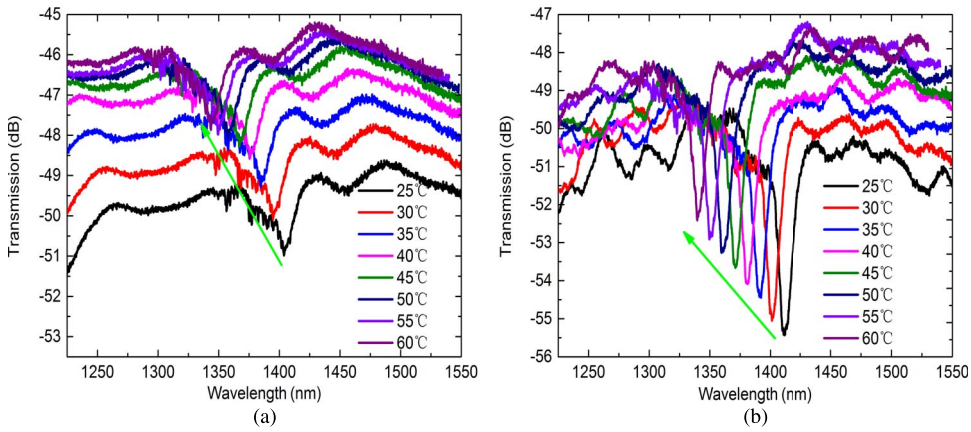

Fig. 8. Transmission spectra of the designed sensor when temperature varies from 25 °C to 60 °C with a step of 5 °C, filled with different volume ratios of ethanol and chloroform. (a) 1:1. (b) 1:2.

TABLE 1

Summary of resonance parameters with volume ratios of ethanol and chloroform 1:1 and 1:2

Temperature (℃)	Resonance Wavelength (nm)		Resonance Loss (dB)	
	1:1	1:2	1:1	1:2
25	1404	1412	2.08	5.10
30	1395	1400	1.88	5.08
35	1384	1391	1.70	5.01
40	1375	1380	1.69	4.86
45	1367	1369	1.63	4.80
50	1357	1360	1.61	4.78
55	1349	1348	1.60	4.48
60	1340	1339	1.58	4.03

In the wavelength interrogation method, the variations of temperature are defected by measuring the shift of the resonance dip $\Delta\lambda_{peak}$. In this case, the wavelength sensitivity in terms of RI units (RIU) is defined as [22]

$$S_\lambda[\text{nm}/^\circ\text{C}] = \Delta\lambda_{peak}/\Delta T. \tag{5}$$

According to (5), the relationship between resonance wavelength and temperature is plotted in Fig. 9(a). The fitting curves can be expressed as $\lambda = 1448.9881 - 1.8262T$ for 1:1 and $\lambda = 1463.4167 - 2.0833T$ for 1:2. The correlations between the fitting results with the experimental results are 0.99862 and 0.99908, respectively, indicating a good linear relationship between the resonance wavelength and temperature. The temperature sensitivity –2.0833 nm/°C is obtained for 1:2, which is comparable to the results of gold nanoparticles selectively filled (–5.5 nm/°C) [21] and silver nanowires filled (2.7 nm/°C) [22] sensors. Fig. 9(b) shows the comparison of the simulated and experimental results at the ratio 1:2, which all present linearly decreasing relations between peak wavelength and temperature. The fitting curve for the simulation results can be expressed as $\lambda = 1449.7381 - 3.1262T$ with correlation of 0.99987, exhibiting a higher temperature sensitivity (–3.1262 nm/°C) and better linear relationship than the experiment. In general, the experimental and simulated results exhibit a good qualitative agreement with little discrepancies in peak wavelength and sensitivity due to the clustering effect and operate error. As described in [20], [28], clustering of nanowires plays an important role and affects the palsmon band location, result in the discrepancy in peak wavelength.

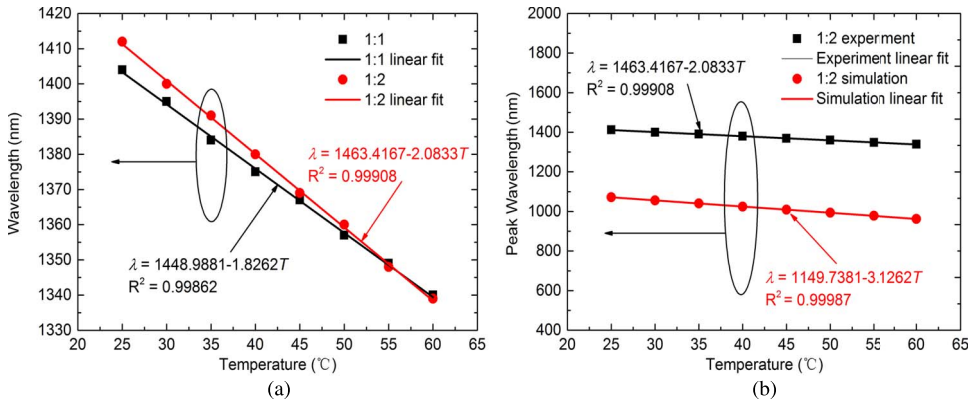

Fig. 9. Relationship between temperature and resonance wavelength. (a) Experiments of 1:1 and 1:2. (b) Experiment of 1:2 and simulation of 1:2.

We use a "figure of merit" to evaluate the experimental results, which is defined as [21]

$$\mathrm{FOM} = S_\lambda(\mathrm{nm}/^\circ\mathrm{C})/\mathrm{FWHM}\ (\mathrm{nm}) \tag{6}$$

where FWHM is the full width at half maximum of the transmission dip. According to equation (6), the FOM we obtained is 0.1572 for 1:2, which is much higher than that of gold colloids and dimethyl sulfoxide filled (0.0762) [21], silver nanowire colloids, and ethanol filled (less than 0.135) [22]. The higher FOM is beneficial for the detection accuracy to get a better performance.

4. Conclusion

In this paper, we present a temperature sensor based on LMA-10 PCF filled with silver nanowire colloids and chloroform. FEM is used to analyze the sensor structure using COMSOL Multiphysics software and the simulated results show that a blue shift is obtained when temperature increase due to the negative thermo-optical coefficients of filling liquid. By changing the volume fractions of silver nanowire colloids and chloroform, the resonance wavelength and resonance intensity can be tuned effectively. A large temperature range from 25 °C to 60 °C at the ratios of 1:1 and 1:2 are detected to investigate the sensor's performance and the high temperature sensitivity −2.08 nm/°C with FOM 0.1572 is obtained, which is comparable to the same type sensors. A significant advancement is made compare with the previous work described in [7]. Firstly, we utilized an all-fiber structure to improve the sensor's mechanical stability, which is also convenient to realize remote sensing by changing the length of the downlead SMF. Next, we had demonstrated the sensor's feasibility both theoretically and experimentally, the FOM is increased from less than 0.135 to 0.1572 with little sacrifice in wavelength sensitivity, which can improve the detection accuracy significantly. This work can provide a reference for developing a high sensitive, real-time, remote sensing and distributed temperature sensor with compact structure.

References

[1] A. Ferrando, E. Silvestre, J. J. Miret, P. Andrés, and M. V. Andrés, "Vector description of higher-order modes in photonic crystal fibers," *J. Opt. Soc. Amer. A, Opt. Image Sci.*, vol. 17, no. 7, pp. 1333–1340, Jul. 2000.
[2] J. N. Dash and R. Jha, "Surface plasmon resonance biosensor based on polymer photonic crystal fibers coated with conducting metal oxide," *IEEE Photon. Technol. Lett.*, vol. 26, no. 6, pp. 595–598, Mar. 2014.
[3] B. T. Kuhlmey, B. J. Eggleton, and D. K. C. Wu, "Fluid-filled solid-core photonic bandgap fibers," *IEEE J. Lightw. Technol.*, vol. 27, no. 11, pp. 1617–1630, Jun. 2009.
[4] Y. Q. Yu *et al.*, "Some features of the photonic crystal fiber temperature sensor with liquid ethanol filling," *Opt. Exp.*, vol. 18, no. 15, pp. 15383–15388, Jul. 2010.
[5] S. J. Qiu, Y. Chen, F. Xu, and Y. Q. Lu, "Temperature sensor based on an isopropanol-sealed photonic crystal fiber in-line interferometer with enhanced refractive index sensitivity," *Opt. Lett.*, vol. 37, no. 5, pp. 863–865, Mar. 2012.

[6] Q. Liu, S. G. Li, H. L. Chen, Z. K. Fan, and J. S. Li, "Photonic crystal fiber temperature sensor based on coupling between liquid-core mode and defect mode," *IEEE Photon. J.*, vol. 7, no. 2, Apr. 2015, Art. no. 4500509.
[7] H. L. Chen, S. G. Li, J. S. Li, Y. Han, and Y. D. Wu, "High sensitivity of temperature sensor based on ultracompact photonics crystal fibers," *IEEE Photon. J.*, vol. 6, no. 6, Dec. 2014, Art. no. 6803006.
[8] T. T. Larsen and A. Bjarklev, "Optical devices based on liquid crystal photonic bandgap fibres," *Opt. Exp.*, vol. 11, no. 20, pp. 2589–2596, Oct. 2003.
[9] J. Villatoro, V. Finazzi, V. P. Minkovich, V. Pruneri, and G. Badenes, "Temperature-insensitive photonic crystal fiber interferometer for absolute strain sensing," *Appl. Phys. Lett.*, vol. 91, no. 9, Aug. 2007, Art. no. 091109.
[10] J. Villatoro, V. Finazzi, and V. Pruneri, "Functional photonic crystal fiber sensing devices," *SPIE*, vol. 8307, no. 1, pp. 1–6, 2011.
[11] P. Zu *et al.,* "A temperature-insensitive twist sensor by using low-birefringence photonic-crystal-fiber-based Sagnac interferometer," *IEEE Photon. Technol. Lett.*, vol. 23, no. 13, pp. 920–922, Jul. 2011.
[12] B. H. Liu, Y. X. Jiang, X. S. Zhu, X. L. Tang, and Y. W. Shi, "Hollow fiber surface plasmon resonance sensor for the detection of liquid with high refractive index," *Opt. Exp.*, vol. 21, no. 26, pp. 32349–32357, Dec. 2013.
[13] Z. K. Fan *et al.,* "High sensitivity of refractive index sensor based on analyte-filled photonic crystal fiber with surface plasmon resonance," *IEEE Photon. J.*, vol. 7, no. 3, Jun. 2015, Art. no. 4800809.
[14] H. W. Zhang *et al.,* "Intracavity absorption multiplexed sensor network based on dense wavelength division multiplexing filter," *Opt. Exp.*, vol. 22, no. 20, pp. 24545–24550, Sep. 2014.
[15] H. L. Chen, S. G. Li, J. S. Li, and Z. K. Fan, "Magnetic field sensor based on magnetic fluid selectively infilling photonic crystal fibers," *IEEE Photon. Technol. Lett.*, vol. 27, no. 7, pp. 717–720, Apr. 2015.
[16] R. Naraoka and K. Kajikawa, "Phase detection of surface plasmon resonance using rotating analyzer method," *Sens. Actuators B Chem.*, vol. 107, no. 2, pp. 952–956, 2005.
[17] A. Hassani and M. Skorobogatiy, "Design of the microstructured optical fiber-based surface plasmon resonance sensors with enhanced microfluidics," *Opt. Exp.*, vol. 14, no. 24, pp. 11616–11621, Nov. 2006.
[18] Y. Peng, J. Hou, Z. H. Huang, and Q. S. Lu, "Temperature sensor based on surface plasmon resonance within selectively coated photonic crystal fiber," *Appl. Opt.*, vol. 51, no. 26, pp. 6361–6367, Sep. 2012.
[19] Q. Liu, S. G. Li, H. L. Chen, J. S. Li, and Z. K. Fan, "High-sensitivity plasmonic temperature sensor based on photonic crystal fiber coated with nanoscale gold film," *Appl. Phys. Exp.*, vol. 8, no. 4, Mar. 2015, Art. no. 046701.
[20] A. Csaki *et al.,* "Nanoparticle layer deposition for plasmonic tuning of microstructured optical fibers," *Small*, vol. 6, no. 22, pp. 2584–2589, Nov. 2010.
[21] Y. Peng *et al.,* "Temperature sensing using the bandgap-like effect in a selectively liquid-filled photonic crystal fiber," *Opt. Lett.*, vol. 38, no. 3, pp. 263–265, Feb. 2013.
[22] Y. Lu, M. T. Wang, C. J. Hao, Z. Q. Zhao, and J. Q. Yao, "Temperature sensing using photonic crystal fiber filled with silver nanowires and liquid," *IEEE Photon. J.*, vol. 6, no. 3, Jun. 2014, Art. no. 6801307.
[23] N. N. Luan *et al.,* "Surface plasmon resonance temperature sensor based on photonic crystal fibers randomly filled with silver nanowires," *Sensors*, vol. 14, no. 9, pp. 16035–16045, Aug. 2014.
[24] Y. Lu *et al.,* "Grapefruit fiber filled with silver nanowires surface plasmon resonance sensor in aqueous environments," *Sensors*, vol. 12, pp. 12016–12025, Aug. 2012.
[25] E. D. Palik, *Handbook of Optical Constants of Solids.* San Diego, CA, USA: Academic, 1985.
[26] X. C. Yang, Y. Lu, M. T. Wang, and J. Q. Yao, "SPR sensor based on exposed-core grapefruit fiber with bimetallic structure," *IEEE Photon. Technol. Lett.*, vol. 28, no. 6, pp. 649–652, Mar. 2016.
[27] Y. Xia *et al.,* "A selectively coated photonic crystal fiber based surface plasmon resonance sensor," *J. Opt.*, vol. 12, no. 1, pp. 74–77, Dec. 2009.
[28] I. Konidakis, G. Zito, and S. Pissadakis. "Silver plasmon resonance effects in $AgPO_3$/silica photonic bandgap fiber," *Opt. Lett.*, vol. 39, no. 12, pp. 3374–3377, Jun. 2014.